Biosensors and Bioelectronics 39 (2013) 76–81

Contents lists available at SciVerse ScienceDirect

Biosensors and Bioelectronics

journal homepage: www.elsevier.com/locate/bios

Supramolecular architecture based on the self-assembling of multiwall carbon nanotubes dispersed in polyhistidine and glucose oxidase: Characterization and analytical applications for glucose biosensing

Pablo R. Dalmasso, María L. Pedano*, Gustavo A. Rivas*

INFIQC, Departamento de Fisicoquímica, Facultad de Ciencias Químicas, Universidad Nacional de Córdoba, Ciudad Universitaria, 5000 Córdoba, Argentina

ARTICLE INFO

Article history:
Received 11 April 2012
Received in revised form
21 June 2012
Accepted 21 June 2012
Available online 28 June 2012

Keywords:
Carbon nanotubes dispersion
Polyhistidine
Glucose oxidase
Layer-by-layer
Self-assembly
Electrochemical glucose biosensor

ABSTRACT

We report for the first time the development of a sensitive and selective glucose biosensor based on the self-assembling of multiwall carbon nanotubes (MWCNTs) dispersed in polyhistidine (Polyhis) and glucose oxidase (GOx) on glassy carbon electrodes (GCE). The supramolecular architecture was characterized by SEM, FT-IR and electrochemical techniques. The optimum multistructure was obtained with five (MWCNT-Polyhis/GOx) bilayers and one layer of Nafion as anti-interferent barrier. The sensitivity at 0.700 V was (1.94 ± 0.03) mA M^{-1} (r=0.9991), with a linear range between 0.25 and 5.00 mM, a detection limit of 2.2 μM and a quantification limit of 6.7 μM with minimum interference from lactose (1.5%), maltose (5.7%), galactose (1.2%), ascorbic acid (1.0%), and uric acid (3.3%). The biocatalytic layer demonstrated to be highly reproducible since the R.S.D. for 10 successive amperometric calibrations using the same surface was 3.6%. The sensitivity of the biosensor after 15 day storage at 4 °C remained at 90% of its original value. The combination of the excellent dispersing properties and polycationic nature of polyhistidine, the stability of the MWCNT-Polyhis dispersion, the electrocatalytic properties of MWCNTs, the biocatalytic specificity of GOx, and the permselective properties of Nafion have allowed building up a sensitive, selective, robust, reproducible and stable glucose amperometric biosensor for the quantification of glucose in milk samples.

© 2012 Elsevier B.V. All rights reserved.

1. Introduction

The development of highly sensitive, selective, rapid, and affordable methodologies to evaluate the quality of foods, drinks and pharmaceutical products, and to quantify analytes of biomedical and environmental interest has received great attention in the last years. Electrochemical biosensors have demonstrated to be an important tool for routine analysis due to their known advantages related to cost, volume, accuracy, response time, simplicity, potential for miniaturization, and sensitivity (Ahmed et al., 2008; Sadik et al., 2009, Sadik and Mwilu, 2010; Trojanowicz, 2009; Vashist et al., 2011; Wang, 2005, 2008; Wilson and Gifford, 2005).

Carbon nanotubes (CNTs) have been largely used for the construction of electrochemical biosensors due to their outstanding properties such as high electrical conductivity, excellent biocompatibility, chemical stability, mechanical strength, fast electron transfer kinetics, high surface to volume ratio, rich electronic polyaromatic structure, resistance towards surface passivation, and the easy immobilization of biomolecules (Agüí et al., 2008; D'Orazio, 2011; Hu et al., 2010; Jacobs et al., 2010; Justino et al., 2010; Menard-Moyon et al., 2010; Vashist et al., 2011). The poor dispersibility of CNTs in most of the solvents due to their strong van der Waals interactions has been a major problem for their use in the development of electrochemical biosensors (Kim et al., 2012). Thus, several strategies have been proposed for dispersing CNTs without disruption of the electronic and mechanical properties of pristine materials, including the successful use of surfactants, binders, biomolecules and polyelectrolytes (Agüí et al., 2008; Hu et al., 2005; Kim et al., 2012; Li et al., 2009; Loginov et al., 2012; Luque et al., 2011; Rivas et al., 2007a, 2007b; Vashist et al., 2011; Wang and Musameh, 2003; Wang et al., 2003).

The aim of the present work is to integrate the excellent properties of multiwall carbon nanotubes (MWCNTs) dispersed in polyhistidine (Polyhis) with the advantages of layer-by-layer (LBL) self-assembling to develop a new supramolecular architecture for glucose biosensing. LBL self-assembly, a technique that involves the alternate adsorption of polyelectrolytes of opposite charge onto conveniently modified solid surfaces through mainly electrostatic interactions, has emerged as a versatile technique for the immobilization of biomolecules (Decher, 1997; Iost and Crespilho, 2012; Lov et al., 1993, Wilson and Gifford, 2005).

* Corresponding authors. Tel.: +54 351 4334169/80; fax: +54 351 4334188.
E-mail addresses: grivas@fcq.unc.edu.ar, mlpedano@fcq.unc.edu.ar (G.A. Rivas).

0956-5663/$ - see front matter © 2012 Elsevier B.V. All rights reserved.
http://dx.doi.org/10.1016/j.bios.2012.06.041

This technique presents enormous advantages, such as simplicity, consumption of small amounts of reagents, rational design of biorecognition layers, the possibility to include different molecules, and minimal denaturation of adsorbed proteins (Iost and Crespilho, 2012; Lin et al., 2011; Shi et al., 2006).

The biosensor proposed in this work is obtained by the alternate adsorption of glucose oxidase (GOx) and MWCNT-Polyhis dispersion at glassy carbon surfaces. In the following sections we present the characterization of the supramolecular multistructure by amperometry, SEM and FT-IR spectroscopy, the optimization of the biosensor and the analytical applications of the resulting biosensing platform.

2. Experimental

2.1. Reagents

D-(+)-glucose (Glu), D-(+)-galactose (Gal), and uric acid (UA) were obtained from Merck. Maltose (Mal) and lactose (Lac) were purchased from Mallinckrodt and Magel S.A., respectively. Glucose oxidase (GOx) (Type X-S, *Aspergillus niger*, EC 1.1.3.4, 158,900 units per gram of solid) and polyhistidine (Polyhis) (catalog number P9386) were obtained from Sigma. Nafion perfluorinated resin solution 5.00% (w/w) (catalog number 274704) was purchased from Aldrich. Absolute ethanol, NaH_2PO_4, Na_2HPO_4 and ascorbic acid (AA) were from Baker. Multiwalled carbon nanotubes (MWCNTs) 15–45 nm diameter and 1–5 μm length were obtained from NanoLab, USA. Other chemicals were analytical reagent grade and used without further purification.

Polyhis, GOx and Nafion solutions were prepared in 75:25 (v/v) ethanol/0.200 M acetate buffer solution pH 5.00, ultrapure water, and absolute ethanol, respectively. The stock solutions of Glu, Gal, Mal, Lac, AA, and UA were prepared in 0.050 M phosphate buffer pH 7.40 before starting each set of experiments. A 0.050 M phosphate buffer solution pH 7.40 was employed as supporting electrolyte. Ultrapure water ($\rho = 18\ M\Omega\ cm$) from a Millipore-MilliQ system was used to prepare all aqueous solutions.

2.2. Apparatus

Electrochemical measurements were performed with a TEQ_02 potentiostat. Glassy carbon electrodes (GCE, CH Instruments, 3 mm diameter) modified with MWCNTs dispersed in Polyhis were used as working electrodes. A platinum wire and Ag/AgCl, 3 M NaCl were used as counter and reference electrodes, respectively. All potentials are referred to the latter. The electrodes were inserted into the electrochemical cell through holes in its Teflon cover. A magnetic stirrer provided the convective transport during the amperometric measurements.

FT-IR spectra were obtained with a Nicolet FTIR spectrometer ($4.0\ cm^{-1}$ resolution, 32 scans) by drop-coating and drying the samples on a ZnSe disk (Pike Technologies, 25×4 mm).

Scanning Electron Microscopy (SEM) images were obtained with a Field Emission Gun Scanning Electron Microscope (FE-SEM, Zeiss, ∑IGMA model). The dispersions were deposited on GCE disks and air dried.

2.3. Preparation of the MWCNT-Polyhis dispersion

The dispersion of MWCNT in Polyhis was obtained by mixing 1.00 mg of MWCNTs with 1.00 mL of $0.25\ mg\ mL^{-1}$ Polyhis solution followed by sonication for 30 min.

2.4. Preparation of the working electrodes

2.4.1. GCE modified with MWCNT-Polyhis dispersion [GCE/MWCNT-Polyhis]

GCEs were polished with alumina slurries of 1.00, 0.30, and 0.05 μm for 1 min each. After polishing, the electrodes were rinsed with water and cycled 10 times in supporting electrolyte between −0.200 V and 0.800 V at $0.100\ Vs^{-1}$. They were modified with the MWCNT-Polyhis dispersion in the following way: an aliquot of 10 μL was dropped on top of the polished GCE and then the solvent was allowed to evaporate at room temperature.

2.4.2. GCE modified with $(MWCNT\text{-}Polyhis/GOx)_n$ [GCE/$(MWCNT\text{-}Polyhis/GOx)_n$]

The GCE/MWCNT-Polyhis was immersed in a $2.00\ mg\ mL^{-1}$ GOx solution for 5 min. To build the multilayers system, 10 μL of MWCNT-Polyhis were dropped on the top of the electrode and allowed to dry. The next steps were the immersion of the resulting electrode in a $2.00\ mg\ mL^{-1}$ GOx solution for 5 min and rinsing with ultrapure water for 5 s. The following layers were obtained by alternating the last two steps.

2.4.3. GCE modified with MWCNT-Polyhis, GOx and $(Polyhis/GOx)_n$ [GCE/MWCNT-Polyhis/GOx/$(Polyhis/GOx)_n$]

The electrodes were prepared in a similar way to GCE/$(MWCNT\text{-}Polyhis/GOx)_n$ except that a $0.25\ mg\ mL^{-1}$ Polyhis solution was used instead of MWCNT-Polyhis dispersion. To build the multilayer system, the electrodes were immersed for 15 min in Polyhis solution and 5 min in GOx solution.

2.4.4. GCE modified with $(MWCNT\text{-}Polyhis/GOx)_n$ and Nafion [GCE/$(MWCNT\text{-}Polyhis/GOx)_n$/Nafion]

The electrode was prepared as described in 2.4.2 and then coated with 10 μL of a 2.50% (w/w) Nafion solution.

2.5. Procedure

Amperometric experiments were performed in a stirred 0.050 M phosphate buffer solution pH 7.40 by applying the desired working potential (0.700 V) and allowing the transient current to reach a steady-state value prior to the addition of the analyte and the subsequent current monitoring. All the experiments were conducted at room temperature.

The FT-IR spectra of Polyhis and GOx were recorded after deposition on a ZnSe disk and drying of the corresponding samples: 25 μL of $0.25\ mg\ mL^{-1}$ Polyhis (prepared in 1.00×10^{-5} M HCl solution) or 50 μL of $2.00\ mg\ mL^{-1}$ GOx (prepared in ultrapure water). To obtain the spectra of the MWCNT-Polyhis deposit, 25 μL of the dispersion were dropped and dried onto the ZnSe window, rinsed with ultrapure water to wash away the acetate ions, and dried again before the FTIR measurement. To obtain the IR spectra of the (MWCNT-Polyhis/GOx) bilayers, 50 μL of $2.00\ mg\ mL^{-1}$ GOx aqueous solution were dropped on the MWCNT-Polyhis modified ZnSe disk and the GOx layer was allowed to assemble for 5 min (as in the biosensor preparation), rinsed with ultrapure water and dried. Subsequent bilayers were obtained by depositing a new layer of MWCNT-Polyhis and repeating the described procedure. The FT-IR spectra containing different quantities of GOx were obtained by depositing GOx aqueous solutions of a different concentration each time, from 0.25 to $3.00\ mg\ mL^{-1}$.

3. Results and discussion

The positively charged Polyhis has demonstrated to be a very efficient dispersing agent for MWCNT and the GCE modified with this dispersion have presented an excellent electrochemical behavior (Dalmasso et al., 2012). Here, we report the use of GCE/MWCNT-Polyhis as a platform to obtain supramolecular multistructures devoted to the quantification of glucose by LBL self-assembling of GOx on (MWCNT-Polyhis) layers. In the following sections we present the characterization of the supramolecular architecture, the optimization of the experimental conditions to obtain the best analytical performance, and the analytical application of the resulting biosensor.

3.1. Effect of GOx concentration and deposition time

The conditions for GOx adsorption at GCE/MWCNT-Polyhis demonstrated to be critical in the performance of the supramolecular architecture devoted to glucose quantification. To optimize this parameter we evaluated the amperometric response of GCE modified with one bilayer of MWCNT-Polyhis and different concentrations of GOx (0.50, 1.00 and 2.00 mg mL^{-1}) at 0.700 V. The results are shown in Fig. S1. The sensitivity of the biosensor enhances with the adsorption time of GOx for 0.50 and 1.00 mg mL^{-1} GOx, while the time for obtaining the maximum sensitivity becomes shorter as the concentration of GOx increases (30 min vs 60 min, respectively), due to a faster screening of the MWCNT-Polyhis charges. In the case of 2.00 mg mL^{-1} GOx solution, the highest sensitivity is obtained between 5 and 15 min adsorption. Longer adsorption times do not improve the sensitivity. Therefore, the best compromise between sensitivity and preparation time is obtained with 2.00 mg mL^{-1} GOx and 5 min adsorption.

3.2. Polyhis versus MWCNT-Polyhis as "polycationic assemblers"

The design of biosensors based on the self-assembling of multilayers relays on the adsorption of molecular layers mainly through electrostatic interactions. GOx is a negatively charged protein under the working conditions (isoelectric point=4.2; He et al., 2009) and needs a positively charged polyelectrolyte/complex/molecule to over-compensate its charge and allow the generation of a multilayered structure. Two different "polycationic assemblers" were used to immobilize GOx: Polyhis and MWCNT-Polyhis dispersion. The response of the resulting biosensors was evaluated at 0.700 V from the sensitivity towards glucose obtained from the H_2O_2 enzimatically generated and the results are summarized in Table S1. When using the MWCNT-Polyhis dispersion as polycationic layer to allow the self-assembling of GOx, the sensitivity to glucose increases with the numbers of GOx layers from 1 to 3. A similar trend was obtained when using Polyhis, although the sensitivities were considerably smaller than those obtained with MWCNT-Polyhis. These results indicate that the MWCNT-Polyhis dispersion is a more suitable matrix for the immobilization of the biocatalytic layer than the polymer alone, mainly attributed to the increment in the surface area provided by the presence of MWCNTs, the interaction with Polyhis wrapping the nanotubes, and a partial direct adsorption of GOx on some remaining exposed areas of MWCNTs (Gutiérrez et al., 2012).

3.3. Effect of the number of (MWCNT-Polyhis/GOx) layers

The influence of the number of (MWCNT-Polyhis/GOx) bilayers on the sensitivity to glucose obtained from amperometric experiments at 0.700 V was evaluated (Fig. S2). The sensitivity increases with the number of bilayers up to the fifth one, to slightly decrease when assembling more bilayers. This effect could be due either to a lower amount of GOx immobilized at the electrode as the number of layer increases, or to a collapse or compaction of the multilayers that gives place to a thicker matrix that restricts the diffusion of glucose and/or the enzymatic product (H_2O_2) within the biocatalytic layer.

3.4. SEM and FT-IR characterization of the supramolecular architecture

SEM images at different magnifications were obtained for 1 and 5 (MWCNT-Polyhis/GOx) bilayers (Fig. S3). As the number of bilayers increases, the CNTs are more agglomerated and the roughness of the surface and porosity increase, originating some channels. When a 2.5% Nafion is present as a final layer (Fig. S4), the surface looks smooth and a thick layer of polymer film can be seen covering the surface.

To characterize the supramolecular multistructure and assess whether the amount of GOx increases proportionally to the number of bilayers, we performed IR spectroscopy studies. Fig. 1 displays the IR spectra of GOx (a), Polyhis (b), Polyhis and GOx previously mixed in solution (c), and GOx assembled on a MWCNTs-Polyhis deposited on ZnSe (d).

The GOx spectrum (Fig. 1a) shows the characteristic bands amide I (1657 cm^{-1}) and amide II (1539 cm^{-1}) due to the peptidic bond. Amide I band of peptides and proteins mainly involves the stretching vibrations of the peptide carbonyl groups. The amide II absorbance band is attributed to the combination of N–H in-plane bending and C–N stretching vibrations of the peptidic bonds. The broad absorbance peak around 3290 cm^{-1} is assigned to N–H stretching vibrations (Simonian et al., 2002).

In the Polyhis spectrum (Fig. 1b) three main peaks can be distinguished in the region from 1400 to 1700 cm^{-1}. The band at 1658 cm^{-1} and the shoulder at 1623 cm^{-1} are assigned to amide I band and stretching vibration between C4 and C5 of the imidazole ring (C4=C5), respectively (El Khoury and Hellwig, 2009). The band at 1534 cm^{-1} is attributed to the amide II band, while the one at 1479 cm^{-1} could be assigned to the amide II band which includes the C–N vibrations. Polyhis spectrum also shows two characteristic bands at 3132 and 3018 cm^{-1}, which could be attributed to N–H stretching vibrations (Simonian et al., 2002).

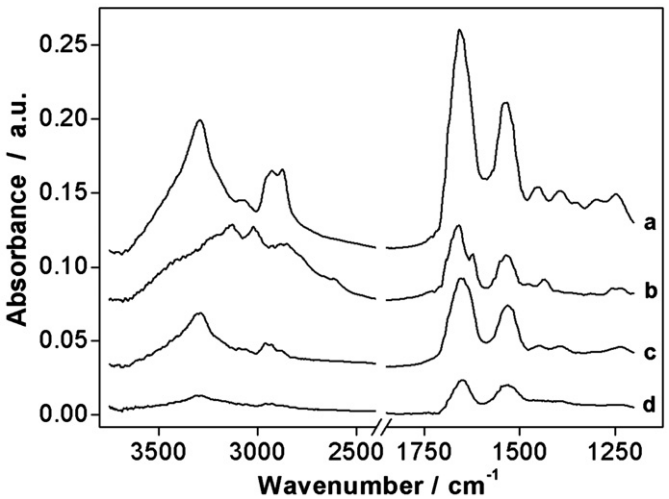

Fig. 1. FT-IR spectrum of (a) GOx, (b) Polyhis, (c) Polyhis and GOx previously mixed in solution, and (d) GOx on MWCNT-Polyhis dispersion. The measurements were performed in triplicate.

From the comparison of Polyhis and GOx spectra, the main differences can be found in the region between 2500 and 3500 cm^{-1}. Therefore, the characteristic absorption band of GOx around 3290 cm^{-1} was selected to quantify the enzyme. In the mid and far IR-domain both Polyhis and GOx spectra exhibit common peptidic bands with exception to a week band at 1299 cm^{-1} present only in the GOx spectrum.

The resulting spectrum of the Polyhis and GOx mixture in solution (Fig. 1c) shows bands characteristics for both polypeptides. The slight shifts of the characteristic absorption bands of GOx (amide I, from 1657 to about 1650 cm^{-1}, and amide II from 1539 to about 1530 cm^{-1}) indicate the successful interaction between the enzyme and Polyhis, and allow to point out that the secondary structure of GOx is retained during the interaction process.

Three well defined peaks, at 3282, 1650 and 1533 cm^{-1}, can be observed in the IR spectrum obtained when GOx is deposited on MWCNT-Polyhis dispersion, which correspond to vibrational modes of GOx (Fig. 1d). These results confirm that GOx can be assembled on MWCNT-Polyhis dispersion and that the immobilized enzyme can preserve its near-native structure (Salimi and Noorbakhsh, 2011).

To evaluate the adsorption of GOx when building the layer-by-layer multistructure, IR spectra were recorded for $(MWCNT\text{-}Polyhis/GOx)_n$ with increasing number of bilayers (n) (Fig. 2A). The main peaks of the enzyme were observed at similar wavenumbers as in Fig. 1c and d, indicating that GOx does not undergo denaturation during the immobilization process. The integrated absorbance (IA) of the band centered around 3290 cm^{-1}, between 3100 and 3500 cm^{-1}, increases linearly as the number of enzyme layers increases (Fig. 2B), confirming the adsorption and retention of GOx on MWCNT-Polyhis after each successive cycle of LBL deposition.

In order to obtain a correlation between the integrated absorbance (IA) at 3290 cm^{-1} and the amount of GOx adsorbed on the multilayer system, we recorded IR spectra for increasing amounts of GOx deposited on the ZnSe tablet. The spectra are shown in Fig. S5A, while the corresponding calibration plot is depicted in Fig. S5B. There is a linear relationship between IA at 3290 cm^{-1} and the amount of protein deposited, the equation for the linear regression being IA (u.a.)$=0.122\times$ m (μg)$+0.099$ ($r=0.995$), where m is the GOx mass deposited. Thus, the estimated amount of GOx assembled after each LBL deposition process (Fig. 2B) can be calculated using this equation and the integrated absorption band for GOx at around 3290 cm^{-1} from the spectra displayed in Fig. 2A. The results reveal that the amount of GOx increases linearly with the number of bilayers, at least up to the seventh bilayer. Therefore, the decrease in sensitivity observed for a number of bilayers higher than 5 (Fig. S2) is not due to a decrease in the amount of GOx immobilized, reinforcing the hypothesis of a diffusional limitation originated by the collapse or compaction of the self-assembled multilayer architecture indicated in Section 3.3.

3.5. Effect of the number of (MWCNT-Polyhis/GOx) layers and the presence of Nafion

One very important aspect from the analytical point of view when developing an amperometric biosensor is the ability to discriminate between the response of the analyte and those for easily oxidizable compounds. AA and UA are the most common interferents for the amperometric detection of bioanalytes due to their low oxidation overvoltages. Different strategies have been proposed to eliminate this interference. Among them, the use of Nafion, a well-known negatively charged polyelectrolyte matrix, that reduces the permeability of negatively charged analytes, has demonstrated to be highly successful (Lukachova et al., 1998; Shankaran et al., 2003).

We evaluate the effect of Nafion as the outer layer of the multistructure on the sensitivity to glucose as a function of the number of bilayers (Fig. 3A) for different concentrations of Nafion: 1.00 (a), 2.50 (b) and 5.00 (c) % (w/w). The profile obtained for 1.00% Nafion indicates that in the presence of this outer layer the signal is smaller than the one obtained for equivalent multistructures without Nafion (compare to Fig. S2). As the concentration of Nafion increases, the sensitivities decrease and the maximum values are reached with lower number of bilayers, demonstrating that the diffusional problems become more important. This effect is critical when $GCE(MWCNT\text{-}Polyhis/GOx)_n$ is covered with 5.00% (w/w) Nafion solution, where a drastic decrease in sensitivity is observed.

Therefore, despite the biosensor without the final layer of Nafion provides the highest amperometric response to glucose, and the increment in the number of (MWCNT-Polyhis/GOx) layers allows a decrease in the interference for AA and UA, the interference of AA and UA (15% and 37%, respectively; not shown) was still high for considering any practical application of the multistructure.

Fig. 3B shows a comparison of the interference percentage for 2.00×10^{-5} M AA (light gray) and 5.00×10^{-5} M UA (dark gray) on the amperometric signal for 1.00×10^{-3} M glucose obtained at 0.700 V as a function of the number of bilayers and the Nafion concentration. In all cases, the increment in Nafion concentration reduces the AA and AU interference. The increase in the number of (MWCNT-Polyhis/GOx) layers also decreases the interference, supporting the hypothesis that, in addition to the repelling effect caused by the Nafion layer, the multilayer system works as a diffusional barrier for these compounds. Therefore, considering

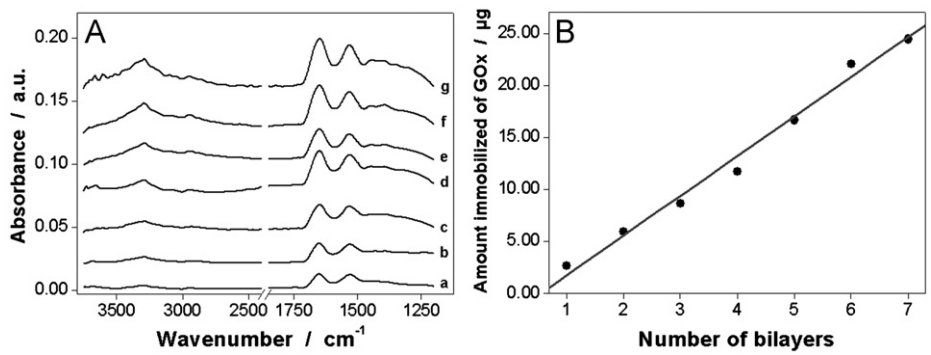

Fig. 2. (A) FT-IR spectra obtained by alternate adsorption of GOx and (MWCNT-Polyhis) layers on a ZnSe disk. (B) Dependence of the amount of GOx adsorbed as a function of the number of self-assembled (MWCNT-Polyhis/GOx) bilayers deposited on a ZnSe window, calculated from the integrated absorbance (IA) between 3100 and 3500 cm^{-1} in the spectra shown in A and the calibration curve in Fig. S5B.

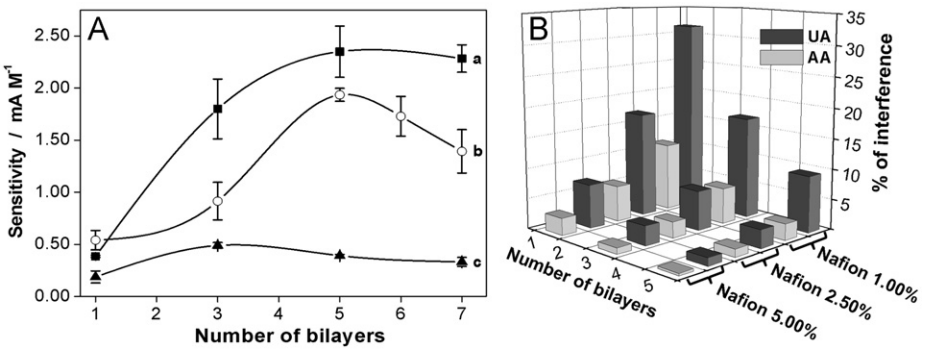

Fig. 3. (A) Dependence of the sensitivity obtained from amperometric recordings after successive additions of glucose on the number of (MWCNT-Polyhis/GOx) bilayers for different concentrations of Nafion deposited on the top of the surface: (a) 1.00%, (b) 2.50%, and (c) 5.00% (w/w). (B) Percentage of interference of ascorbic acid (2.00×10^{-5} M) and uric acid (5.00×10^{-5} M) on the amperometric signal obtained after addition of 1.00×10^{-3} M glucose as a function of the number of (MWCNT-Polyhis/GOx) layers and the Nafion concentration. The percentage of interference was obtained as $(i_{int}/i_{glu}) \times 100$, where i_{int} and i_{glu} are the currents obtained after addition of the given interferent and the current for the hydrogen peroxide enzymatically generated from glucose, respectively. Working potential: 0.700 V. Supporting electrolyte: 0.050 M phosphate buffer solution pH 7.40.

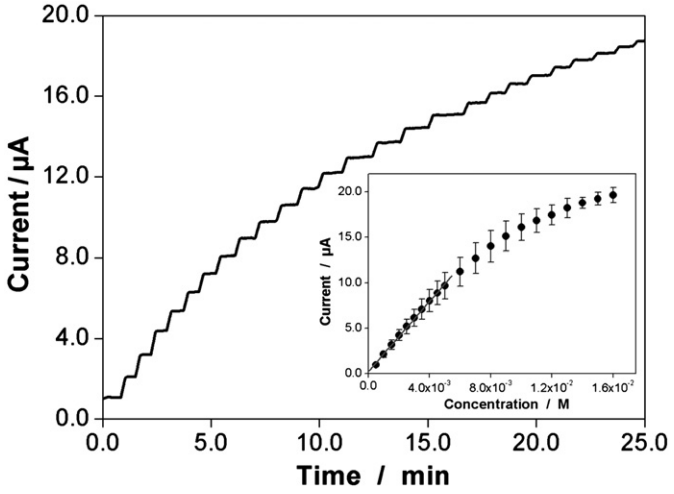

Fig. 4. (A) Amperometric response at GCE/(MWCNT-Polyhis/GOx)$_5$/Nafion for the addition of 5.00×10^{-4} M glucose. Working potential: 0.700 V. Inset: Calibration plot obtained from the average of seven amperometric recordings like the one shown in (A). Other conditions, as in Fig. 3.

the results shown in Fig. 3A and B and the high percentage of interference obtained for the multilayers without Nafion, it is evident that is necessary to reach a compromise between obtaining the highest sensitivity and the lowest interference. This compromise is obtained with five (MWCNT-Polyhis/GOx) bilayers and a 2.50% (w/w) Nafion layer.

In summary, the optimal experimental parameters selected for building the glucose biosensor were: adsorption of 2.00 mg mL^{-1} GOx for 5 min, five (MWCNT-Polyhis/GOx) layers, and the presence of an outer film of 2.50% (w/w) Nafion.

3.6. Analytical performance of the biosensor

Fig. 4A depicts the amperometric current-time recording obtained with GCE/(MWCNT-Polyhis/GOx)$_5$/Nafion for successive additions of 5.00×10^{-4} M glucose obtained under the optimum conditions. The corresponding calibration plot is shown in the inset. The amperometric profile shows a well-defined response, being 12 s the time necessary to reach the 95% of the steady-state current. The inset shows a linear relationship between the oxidation current and the glucose concentration in the range from 2.50×10^{-4} M to 5.00×10^{-3} M with an average sensitivity of (1.94 ± 0.03)mA M^{-1} and a correlation coefficient of 0.9991 (values obtained from seven different biosensors and four different dispersions). The detection limit was 2.2 µM (taken as 3.3 σ/S, where σ is the standard deviation of the blank signal and S, the sensitivity), and the quantification limit, 6.7 µM (taken as 10 σ/S).

The K_m^{app} value is smaller than the K_m reported for the native GOx in solution, suggesting that the environment where GOx is immobilized allows higher enzymatic activity and higher affinity towards glucose than GOx in solution (see Supplementary Information).

One very important analytical parameter for practical applications is the stability of the biosensor. The short-term stability of GCE/(MWCNT-Polyhis/GOx)$_5$/Nafion demonstrated to be excellent, since the R.S.D. for 10 successive amperometric calibrations for glucose performed at 0.700 V using the same surface (implying more than 90 min of continuous use) was 3.6% (not shown). For evaluating the long-term stability, the biosensor was stored at 4 °C when not in use. The stability was examined through the sensitivity towards glucose obtained from periodic amperometric measurements at 0.700 V. The sensitivity remained constant over the first ten days, to decrease around 10% of the original value after 15 days. These results suggest that the supramolecular architecture provides a favorable microenvironment for retaining the functional properties of GOx.

The selectivity of the current glucose biosensor, considering possible interfering species that can be present in a milk matrix, was evaluated by measuring the amperometric response at 0.700 V to successive additions of 2.00×10^{-3} M Lac, 5.00×10^{-4} M Mal, 1.00×10^{-3} M Gal, 1.00×10^{-5} M AA, 2.00×10^{-5} M UA, and 1.00×10^{-3} M glucose, being the interference percentages 1.5% for Lac, 5.7% for Mal, 1.2% for Gal, 1.0% for AA, and 3.3% for UA. These results reveal the high selectivity of the proposed glucose biosensor (Fig. S6).

Compared to other MWCNT-based glucose biosensors shown in Supplementary Table S2, our biosensor possesses: (a) a good sensitivity which is better than the reported by Wang et al. (2007, 2011), Wen et al. (2009), and Yao and Shiu (2007), (b) a wide linear range, comparable to most of the ones indicated in Table S2 and even better than some of them, and (c) an excellent detection limit which is the lowest of those summarized in Table S2, with exception to the one reported by Li et al. (2011). Additional advantages of our biosensor are: (a) the use of well-dispersed pristine MWCNTs without the need of covalent functionalization for self-assembling GOx, (b) their excellent long-term stability, and (c) their ability to determine glucose even in the presence of several interfering analytes. Therefore, the analytical characteristics of the proposed biosensor allow emphasizing that it could

be a valuable tool for routine analysis of glucose and quality control in dairy and food industries.

In order to evaluate the practical application of the GCE/(MWCNT-Polyhis/GOx)$_5$/Nafion biosensor, the electrode was used to determine the glucose content in baby formula milk samples ("Crecer 1" milk for babies from 0 to 6 months, Argentine dairy company "La Serenísima"). Nine determinations from four samples of the milk (diluted 1:40 with 0.050 M phosphate buffer pH 7.40) yielded a glucose concentration of $(3.6 \pm 0.2) \times 10^{-2}$ M, which agrees very well with that reported by "La Seresísima" company (3.9×10^{-2} M). This excellent correlation demonstrates that GCE/(MWCNT-Polyhis/GOx)$_5$/Nafion is a successful analytical tool for the determination of glucose in such a complex medium as milk.

4. Conclusions

We have demonstrated the advantages of using the dispersion of MWCNT in Polyhis to successfully assemble GOx. The combination of the outstanding dispersing properties and polycationic nature of polyhistidine, the stability of the MWCNT-Polyhistidine dispersion, the electrocatalytic properties of MWCNTs, the biocatalytic specificity of GOx, and the permselective properties of Nafion, allowed the successful self-assembly of (MWCNTs-Polyhis/GOx) multilayers to build up a sensitive, selective, robust, reproducible and stable glucose amperometric biosensor.

The new platform represents an interesting alternative to develop biosensors taking advantage of the MWCNTs dispersed in Polyhis without the need of previous treatment of the CNTs to generate different functional groups or covalent attachment of bioactive groups.

Acknowledgements

The authors thank CONICET, ANPCyT, SECyT-UNC, MINCyT-Córdoba for the financial support. P.R.D. thanks CONICET for the postdoctoral fellowship.

Appendix A. Supplementary Information

Supplementary data associated with this article can be found in the online version at http://dx.doi.org/10.1016/j.bios.2012.06.041.

References

Agüí, L., Yáñez-Sedeño, P., Pingarrón, J.M., 2008. Analytica Chimica Acta 622, 11–47.
Ahmed, M.U., Hossain, M.M., Tamiya, E., 2008. Electroanalysis 20, 616–626.
Dalmasso, P.R., Pedano, M.L., Rivas, G.A., 2012. Analytica Chimica Acta 710, 58–64.
Decher, G., 1997. Science 29, 1232–1237.
D'Orazio, P., 2011. Clinica Chimica Acta: International Journal of Clinical Chemistry 412, 1749–1761.
El Khoury, Y., Hellwig, P., 2009. Journal of Biological Inorganic Chemistry 14, 23–34.
Gutiérrez, F., Rubianes, M.D., Rivas, G.A., 2012. Sensors and Actuators B 161, 191–197.
He, C., Liu, J., Xie, L., Zhang, Q., Li, C., Gui, D., Zhang, G., Wu, C., 2009. Langmuir 25, 13456–13460.
Hu, C., Zhang, Y., Bao, G., Zhang, Y., Liu, M., Wang, Z.L., 2005. The Journal of Physical Chemistry B 109, 20072–20076.
Hu, L., Hecht, D.S., Grüner, G., 2010. Chemical Reviews 110, 5790–5844.
Iost, R.M., Crespilho, F.N., 2012. Biosenors and Bioelectronics 31, 1–10.
Jacobs, C.B., Peairs, M.J., Venton, B.J., 2010. Analytica Chimica Acta 662, 105–127.
Justino, C.I.L., Rocha-Santos, T.A., Duarte, A.C., Rocha-Santos, T.A., 2010. Trends in Analytical Chemistry 29, 1172–1183.
Kim, S.W., Kim, T., Kim, Y.S., Choi, H.S., Lim, H.J., Yang, S.J., Park, C.R., 2012. Carbon, 3–33.
Li, W., Yuan, R., Chai, Y., Zhong, H., Wang, Y., 2011. Electrochimica Acta 56, 4203–4208.
Li, Z., Wu, Z, Li, K., 2009. Analytical Biochemistry 387, 267–270.
Lin, A.-J., Wen, Y., Zhang, L.-J., Lu, B., Li, Y., Jiar, Y.-Z., Yang, H.-F., 2011. Electrochimica Acta 56, 1030–1036.
Loginov, M., Lebovka, N., Vorobiev, E., 2012. Journal of Colloid and Interface Science 365, 127–136.
Lov, Y., Decher, G., Mohwald, H., 1993. Langmuir 9, 481–486.
Lukachova, L.V., Karyakin, A.A., Ivanova, Y.N., Karyakina, E.E., Varfolomeyev, S.D., 1998. Analyst 123, 1981–1985.
Luque, G.L., Ferreyra, N.F., Granero, A., Bollo, S., Rivas, G.A., 2011. Electrochimica Acta 56, 9121–9126.
Menard-Moyon, C., Kostarelos, K., Prato, M., Bianco, A., 2010. Chemistry and Biology 17, 107–115.
Rivas, G.A., Rubianes, M.D., Pedano, M.L., Ferreyra, N.F., Luque, G.L., Rodríguez, M.C., Miscoria, S.A., 2007a. Electroanalysis 19, 823–831.
Rivas, G.A., Rubianes, M.D., Rodríguez, M.C., Ferreyra, N.F., Luque, G.L., Pedano, M.L., Miscoria, S.A., Parrado, C., 2007b. Talanta 74, 291–307.
Sadik, O.A., Aluoch, A.O., Zhou, A., 2009. Biosensors and Bioelectronics 24, 2749–2765.
Sadik, O., Mwilu, S.K., 2010. Electrochimica Acta 55, 4287–4295.
Salimi, A., Noorbakhsh, A., 2011. Electrochimica Acta 56, 6079–6105.
Shankaran, D.R., Uehara, N., Kato, T., 2003. Biosensors and Bioelectronics 18, 721–728.
Shi, H.B., Yang, Y., Huang, J.D., Zhao, Z.X., Xu, X.H., Anzai, J.I., Osa, T., Chen, Q., 2006. Talanta 70, 852–858.
Simonian, A.L., Revzin, A., Wild, J.R., Elkind, J., Pishko, M.V., 2002. Analytica Chimica Acta 466, 201–212.
Trojanowicz, M., 2009. Analytica Chimica Acta 653, 36–58.
Vashist, S.K., Zheng, D., Al-Rubeaan, K., Luong, J.H.T., Sheu, F.-S., 2011. Biotechnology Advances 29, 169–188.
Wang, H.J., Zhou, C.M., Peng, F., Yu, H., 2007. International Journal of Electrochemical Science 2, 508–516.
Wang, J., 2005. Analyst 130, 421–426.
Wang, J., 2008. Chemical Reviews 108, 814–825.
Wang, J., Musameh, M., 2003. Analytical Chemistry 75, 2075–2079.
Wang, J., Musameh, M., Lin, Y., 2003. Journal of the American Chemical Society 125, 2408–2409.
Wang, Y., Liu, L., Li, M., Xu, S., Gao, F., 2011. Biosensors and Bioelectronics 30, 107–111.
Wen, Z., Ci, S., Li, J., 2009. Journal of Physical Chemistry C 113, 13482–13487.
Wilson, G.S., Gifford, R., 2005. Biosensors and Bioelectronics 20, 2388–2403.
Yao, Y.-L., Shiu, K.-K., 2007. Electrochimica Acta 53, 278.